Soft Matter

Competing Polymer-Substrate Interactions Mitigate Random Copolymer Adsorption

Journal:	*Soft Matter*
Manuscript ID	SM-ART-07-2018-001433.R1
Article Type:	Paper
Date Submitted by the Author:	11-Aug-2018
Complete List of Authors:	Davis, Mary; Princeton University, Chemical and Biological Engineering Zuo, Biao; Zhejiang Sci-Tech University, Deoartment of Chemistry Priestley, Rodney; Princeton University, Chemical and Biological Engineering

Soft Matter

ARTICLE

Competing Polymer-Substrate Interactions Mitigate Random Copolymer Adsorption

Received 00th January 20xx,
Accepted 00th January 20xx

DOI: 10.1039/x0xx00000x

www.rsc.org/

Mary J. B. Davis,[a] Biao Zuo [a,b] and Rodney D. Priestley* [a,c]

Annealing a supported polymer film in the melt state, a common practice to relieve residual stresses and erase thermal history, can result in the development of an irreversibly adsorbed nanolayer. This layer of polymer chains physically adsorbed to the substrate interface has been shown to influence thin film properties such as viscosity and glass transition temperature. Its growth is attributed to many simultaneous interactions between individual monomer units and the substrate stabilizing chains against desorption. A better understanding of how these specific polymer-substrate interactions influence the growth of the adsorbed layer is needed, particularly given how strongly the properties of geometrically confined polymeric systems are impacted by interfaces. Here, we use homopolymers and random copolymers of styrene and methyl methacrylate to form adsorbed layers and examine the influence of chemical composition and the resulting polymer-substrate interactions on adsorbed layer growth and structure. Ellipsometric measurements reveal a non-monotonic trend between composition and thickness of the adsorbed layers that is inconsistent with the behavior normally exhibited by random copolymers, being intermediate to their respective homopolymers. We examine this trend in terms of plateau thickness and growth kinetics at two different annealing temperatures and propose a mechanism for how different polymer-substrate interactions combine to influence adsorption when copolymer films are annealed. By introducing compositional heterogeneity, this mechanism extends the study of irreversible adsorption to complex chemistries and provides for a more general understanding of how annealing should be accounted for in the proper selection and processing of polymer thin films for applications in nanotechnology.

Introduction

Polymers confined to nanometre length scales are of rising importance as technology is driven to increasingly smaller dimensions. In confined geometries, polymers have been shown to exhibit dynamic,[1–3] mechanical,[4–8] and thermal[9–13] properties much different than their corresponding bulk values. One such geometry, a polymer thin film, has many industrial applications in membrane,[14,15] electronic,[16,17] and drug delivery[18] technologies and has proven to be an excellent model system to study the influence of interfaces on material properties. These interfaces, whether they be with air (free surface),[12,19,20] another polymer,[21,22] or a solid substrate,[23] are largely believed to contribute to the observed changes in the properties of confined polymers. Many studies have shown that free surfaces act to greatly enhance polymer mobility and reduce the glass transition temperature (T_g).[19,24,25] Additionally, attractive interactions between polymer and substrate result in a reduction in mobility and increase in T_g in supported films.[23,26] These effects, originating at interfaces, have been shown to penetrate tens of nanometres into a film, thus forming gradients in local properties.[2,11] As a result of the direct competition of interfacial influences, the magnitude, direction, and onset of observed deviations from bulk behaviour with film thickness vary depending on polymer composition[9,26,27] and interaction strength with supporting substrates.[23,28] For example, polystyrene (PS), which weakly interacts with a silicon substrate, exhibits large negative deviations from its bulk T_g below 40 nm film thickness[11,12] due to enhanced mobility at the free surface.[29,30] Alternatively, silicon substrates have hydrogen-bonding interactions with poly(methyl methacrylate) (PMMA) and poly(2-vinylpyridine) (P2VP) films that create positive deviations in film T_g with reduced thickness, below a critical value.[28] However, eliminating the potential for hydrogen bonding, by removing or coating the substrate, allows the free surface effect to dominate, resulting in negative deviations in T_g for PMMA.[23,31] Random copolymers exhibit thickness-dependent T_g intermediate to their respective homopolymers,[9,32] which allows for the control of thin film T_g by tuning composition. Park *et al.* observed random copolymer confinement behaviour reflective of composition by ellipsometry.[32] P(S-*r*-

[a] *Department of Chemical and Biological Engineering, Princeton University, Princeton, NJ 08544, USA*
[b] *Department of Chemistry, Key Laboratory of Advanced Textile Materials and Manufacturing Technology of the Education Ministry, Zhejiang Sci-Tech University, Hangzhou 310018, China.*
[c] *Princeton Institute for the Science and Technology of Materials, Princeton University, Princeton, NJ 08544, USA*
† Footnotes relating to the title and/or authors should appear here.
Electronic Supplementary Information (ESI) available: [details of any supplementary information available should be included here]. See DOI: 10.1039/x0xx00000x

MMA) with a majority S component showed negative deviations from bulk T_g, and the magnitude of these deviations decreased with higher MMA content. They described these deviations with a parallel-type additive interaction parameter, in which the polymer component with lower substrate interaction strength (styrene) dominated confinement behaviour. They found this relation held for P2VP-*co*-PS as well. Mundra *et al.* also measured a composition-dependent T_g-confinement effect in P(S-*r*-MMA) by intrinsic fluorescence, showing a more evenly-balanced influence from component polymers.[9]

Annealing polymer thin films in the melt state is often an essential step in their preparation in order to remove thermal history, solvent, and stresses introduced during processing.[33] However, in addition to its role in erasing thermal history, annealing above T_g can result in the growth of an irreversibly adsorbed nanolayer.[34–40] This layer of adsorbed polymer chains has been shown to grow in thickness and evolve in dynamic properties with annealing time,[38] while impacting film properties such as diffusion[41], mobility,[41–43] viscosity,[44] and T_g.[38,45–47] Recently, we used a fluorescence bilayer technique to selectively measure T_g of exposed and buried PS adsorbed layers.[48] These geometries enabled isolation of the impact of the free surface on adsorbed layer T_g and revealed that it was suppressed at later stages of growth due to stronger chain adsorption at the substrate dominating over free surface effects. Perez-de-Eulate *et al.* further demonstrated the ability of irreversible adsorption to largely erase a dramatic free surface effect[27] through the recovery of bulk T_g in poly(*tert*-butylstyrene) (PtBS) thin films with extended annealing.[49]

Since the development of adsorbed nanolayers has been closely associated with deviations from bulk behaviour in thin films,[38,41,44,48,49] understanding the mechanism and kinetics of their growth gives insight into how annealing can impact confined polymer properties. Adsorbed layers have been isolated through solvent washing and experimentally characterized in terms of thickness,[38,48,50] density,[39,40] surface topography,[39,48] and T_g.[38,45,48] These measurements enabled elucidation of their equilibrium thickness,[48,51–53] architecture,[39,40] and growth mechanism.[39,50,53,54] With increased annealing time, adsorbed layers gradually thicken toward a quasi-equilibrium, or plateau, thickness.[51] Experiments and simulations on homopolymer systems have shown that this thickness (h_p) scales with chain length following random walk statistics,[51,52] with the scaling factor depending on polymer-substrate interactions.[51,53] Chains adsorb in a combination of trains (consecutive segments adsorbed to the substrate), loops (unadsorbed stretches with bound segments on either end), and tails (unadsorbed sections with only one adsorbed end).[40] Koga and co-workers focused on the characterization of adsorbed chain conformations resulting from different stages of growth and identified two distinct sublayers: a tightly-bound, densely-adsorbed "flattened layer" and a "loosely-bound layer".[39,40] Jiang *et al.* studied the growth of PS, PMMA, and P2VP flattened layers further, observing an increase in h_p with increasing polymer-substrate interaction strength.[39]

The growth of PS adsorbed layers from the melt state is commonly believed to follow two kinetic regimes: fast growth at short times, corresponding to chains pinning to a largely uncovered substrate, and slow surface-coverage limited growth at long times, as chains adsorb through initially attached chains and rearrange. Jiang *et al.* further described the fast growth regime at early stages of adsorption as a race between zipping down of tightly-bound chains and diffusion-limited adsorption of loosely bound chains.[39] This two-stage mechanism is consistent with the bimodal growth reported for chains adsorbing from solution.[39,55] Housmans *et al.* found both these stages to be dependent on annealing temperature and polymer molecular weight.[50] Simavilla *et al.* later proposed that annealing temperature impacts the growth of homopolymer adsorbed layers from two distinct contributions: thermal fluctuations of the polymer chain and polymer-substrate interaction strength.[53] Changes in polymer chain fluctuation with temperature depend on the polymer's thermal activation energy of segmental motion (E_a), which was reflected by an Arrhenius temperature dependence of adsorption rate. Individual segmental interaction strength with the substrate was on the order of ~ k_BT, consistent with findings in adsorption from solution studies.[56] Simavilla *et al.* argued that this temperature dependence was much lower than that of E_a, and therefore annealing temperature (T_{ann}) should have a much larger impact on kinetics than h_p. They demonstrated that h_p did not change significantly with T_{ann} for several homopolymer systems.

Despite the well-established influence of polymer-substrate interactions and the growing appreciation for the role of irreversible adsorption in determining confined film properties, considerable investigation is still needed into how these influences are interrelated. While there has been limited work examining polymer-substrate interactions as related to homopolymer adsorbed layer growth,[39,51,53] there has been no examination of how different polymer-substrate interactions combine in the growth of random copolymer adsorbed layers. Extending the study of irreversible adsorption to polymers with heterogeneous compositions is critical in determining its generality and application to more complex systems.

Here, we study model systems of PS, PMMA, and P(S-*r*-MMA) spanning the full range of composition. This set of polymers is advantageous fundamentally because it allows for the comparison between two different polymer-substrate interactions: Van der Waals in the case of PS and hydrogen bonding in the case of PMMA.[57] Additionally, P(S-*r*-MMA) brushes are often used to modify substrates for PS-*b*-PMMA block copolymer films,[58,59] which are of particular interest in lithography.[16] Through the use of this polymer series, we investigate the impact of specific polymer-substrate interactions on adsorbed layer growth and how they compete in the irreversible adsorption of random copolymers. We find that, unlike with their T_g confinement behaviour (also strongly tied to interfacial interactions), the growth metrics of P(S-*r*-MMA) adsorbed layers are not intermediate to those of PS and PMMA. Rather, h_p is dictated by the degree of compositional heterogeneity and adsorption kinetics are heavily biased

Table 1. Specifications for random copolymers synthesized via free radical polymerization.

Polymer Name	Mole Fraction MMA, x_{MMA}	w_{MMA}	M_w (kg/mol)	$Đ$	T_g (K)	R_g (nm)
PS	0	0	109	1.8	378	9.2
P(S-*r*-MMA) (75:25)	0.25	0.24	99	1.7	376	
P(S-*r*-MMA) (48:52)	0.52	0.51	109	2.0	377	
P(S-*r*-MMA) (27:73)	0.73	0.72	105	2.0	385	
PMMA	1	1	119	2.2	393	9.2

Composition was measured via ^{1}H-NMR. Molecular weight and $Đ$ were measured via SEC. T_g was measured via DSC. R_g was calculated from M_w following empirical relations described in the SI.

towards those of PMMA. We use these results to propose a copolymer adsorption mechanism in which differences in adsorption density and polymer-substrate attraction combine to create a barrier to growth with increasing compositional heterogeneity.

Experimental Methods

Polymer Synthesis and Characterization

Polymers used in this study were synthesized via free radical polymerization of styrene (S) and methyl methacrylate (MMA), both purchased from Sigma-Aldrich. Inhibitors were removed by running these monomers through a column packed with aluminium oxide prior to their use. Relative feed ratios of S and MMA were selected for desired copolymer composition, using reactivity ratios of 0.49 for both S and MMA.[60] Reactions were conducted without additional solvent at 348 K under nitrogen with precise concentrations of benzoyl peroxide (Sigma-Aldrich) initiator to control molecular weight. Copolymer chain compositional uniformity was maintained by restricting the reactions to <15% conversion to avoid drift, and it was confirmed by comparing the composition of polymers synthesized with different reaction times (see SI). Synthesized polymers were dissolved in toluene (Fisher Chemical) and precipitated in methanol (Fisher Chemical) three to four times to remove unreacted monomer, as confirmed by ^{1}H-NMR.

Table 1 summarizes the characterization data obtained for polymers in this study. Copolymers are referred to by their molar composition (X:Y) where X is the mol % S and Y is the mol % MMA. Composition was determined from ^{1}H-NMR spectra by comparing aliphatic and aromatic proton signatures (see SI). Molecular weight was measured via Size Exclusion Chromatography in tetrahydrofuran (THF) against PS standards. Weight average molecular weight (M_W) was determined for each polymer from light scattering data analysed using composition-weighted dn/dc values;[61] homopolymer values were 0.0818 mL/g for PMMA[62] and 0.189 mL/g for PS.[63] Dispersity, $Đ$, was determined from differential refractive index data and used to calculate M_N. The M_W of all polymers were within 10 % of 108 kg/mol in order to reduce the effect of molecular weight on our results. T_g was determined by Differential Scanning Calorimetry (DSC) on a TA Instruments Q2000 DSC, measured as the onset of T_g upon second heating at 10 K/min after cooling at 2.5 K/min. R_g for PS and PMMA were determined from empirical relations, described in the SI.

Adsorbed Layer Preparation

Polymer films 200 ± 20 nm thick were spin-coated from dilute solution onto piranha-treated silicon (wafers were immersed in 70:30 H_2SO_4:H_2O_2 for ~30 minutes and rinsed with deionized H_2O). Films were then annealed at a given temperature (T_{ann}) under 10^{-2} torr vacuum for set lengths of time (t_{ads}) to promote the growth of adsorbed layers. When annealing films relative to their bulk T_g, T_{ann} was: 423 K for PS, P(S-*r*-MMA) (75:25), and P(S-*r*-MMA) (48:52); 430 K for P(S-*r*-MMA) (27:73); and 438 K for PMMA. Those temperatures will be referred to as T_g + 45 K throughout the remainder of the text. Adsorbed layers were then isolated through a series of three rinsing and 10-minute soaking steps in toluene. Fresh toluene was used for each step. These isolated adsorbed layers were then dried overnight at room temperature under vacuum to remove any residual solvent before characterization.

Adsorbed Layer Thickness Measurement

All adsorbed layer characterization was conducted at room temperature. Adsorbed layer thickness was determined using a Woollam M2000 Spectroscopic Ellipsometer. Each sample was measured at a 65° angle at 3 different locations near the centre of the film, each 0.3 cm apart. Δ and Ψ data for wavelength range 400 - 1680 nm were fit to a Cauchy model for transparent films. Cauchy model parameters were fixed and determined for each polymer by averaging fitted measurements of several thicker films, as has been shown previously.[48,50] Native oxide layer thickness was measured on bare substrates prior to spin coating and fixed for each sample when measuring adsorbed layer thickness, thus reducing the likelihood of correlation between measurement of the native oxide layer and adsorbed layer. The ability of these models to accurately report thickness of adsorbed layers was verified through comparisons with atomic force microscopy measurements (see SI).

Results and Discussion

Bulk and Confined T_g of P(S-*r*-MMA)

The copolymers synthesized for this investigation exhibited an asymmetric trend in bulk T_g with composition, as shown by the orange circles in Figure 1. P(S-*r*-MMA) exhibited T_g within 2 K of PS until its MMA weight fraction, w_{MMA}, increased above ~

0.5. The T_g of copolymers with $w_{MMA} > 0.5$ increased rapidly and approximately linearly with w_{MMA} until reaching that of PMMA. This data set was supplemented by additional P(S-*r*-MMA) samples, synthesized via the same method with different monomer feed ratios, to clarify the trend with composition. P(S-*r*-MMA) is a known exception to the Fox equation,[64] shown by the orange line in Figure 1, exhibiting a clear negative deviation. Other consistent data sets, taken from the literature, are shown by the green triangles[32] and purple squares.[65] This large deviation from the Fox equation has been studied in greater detail elsewhere and was attributed to contributions from dyad and triad sequences along the copolymer chains.[32,66,67] These sequences are particularly important in PMMA homopolymers, as tacticity has been shown to have a large impact on its bulk T_g and confinement behavior.[68,‡] Despite the influence of these chain sequences on the T_g of bulk P(S-*r*-MMA), they do not appear to impact the T_g of P(S-*r*-MMA) thin films, which reported T_g deviations proportional to their composition.[9,32] Dominated by interfacial influences rather than chain sequences, P(S-*r*-MMA) confined T_g was attributed to the balance between S and MMA contributions to specific interactions at the substrate (Van der Waals for S and hydrogen-bonding from MMA) and free surface effects.[9,32]

Irreversible adsorption is also an interface-driven phenomena and thus should not be strongly impacted by the chain sequences that dictate bulk T_g. Changes in T_g of PS[38,45,48] and PtBS[49] homopolymer films with annealing have been strongly correlated with the growth of adsorbed layers, but this has not been extended to systems with competing substrate interactions. Examining the irreversible adsorption of P(S-*r*-MMA) presents the opportunity to compare the impact of polymer-substrate interactions on adsorption and confined T_g as well as infer how annealing could impact confinement behaviour in copolymer thin films.

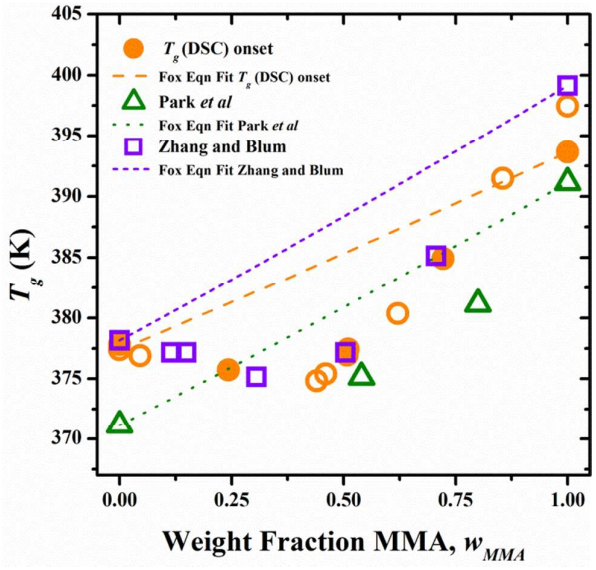

Figure 1. Glass transition temperatures of a series of P(S-*r*-MMA) polymers deviate from the Fox equation[64] and show an asymmetric trend with composition. Polymers synthesized via free radical polymerization are shown in orange circles. Closed circles represent polymers used in this study; open circles are from additional polymers synthesized by the same method as described above are included to show a more complete composition trend. Literature values from Park *et al.*[32] (green triangles) and Zhang and Blum[65] (purple squares) are included and also display an asymmetric trend.

Composition Effects on Adsorbed Layer Plateau Thickness

As described previously, irreversible adsorption has been shown to progress with annealing time, and PS, P(S-*r*-MMA), and PMMA adsorbed layers followed the standard growth pattern. Figure 2 plots adsorbed layer thickness for each polymer as a function of time annealed (t_{ads}) at T_g + 45 K prior to isolation through solvent leaching. The considerably thinner adsorbed layers made by the copolymers, reaching a minimum in P(S-r-MMA) (48:52), were immediately evident and were quantified by h_p. The differences in h_p between these polymers, despite similar M_W, indicate a composition-driven effect. However, the decrease of h_p with increasing heterogeneity, indicated by the non-monotonic trend with composition shown in Figure 3a, provides an interesting contrast to the composition-dependent deviations of confined T_g.[9,32] This difference in behaviour suggests that the close association of adsorption with T_g in homopolymers[38,48,49] does not hold for copolymers and that copolymer h_p is impacted by additional factors that disrupt its direct increase with polymer-substrate interactions (*i.e.,* MMA content).[53] We note that, unlike when comparing adsorbed layer thickness (h_{ads}) for a given polymer,[69] the relative thicknesses of these adsorbed layers cannot be taken to be directly reflective of adsorbed amount (since the proportionality between adsorbed amount and h_{ads} varies for each polymer). This adsorbed amount is associated with changes in polymer properties with annealing.[38]

It is important to note that P(S-*r*-MMA) (27:73) and PMMA were annealed at higher absolute temperature to maintain the constant difference between T_{ann} and bulk T_g. Johnson *et al*. reported a temperature dependence of segmental interactions, stronger with MMA than PS,[56] which might imply that this higher T_{ann} was solely responsible for the non-monotonic trend in h_p. However, as indicated by the stars in

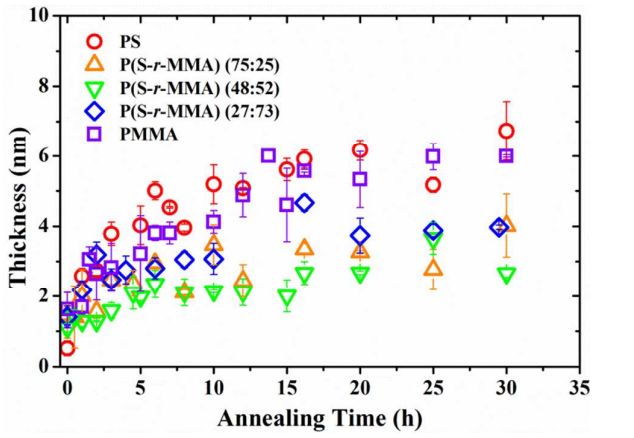

Figure 2. The growth of PS, P(S-*r*-MMA), and PMMA irreversibly adsorbed layers at T_g + 45 K reveals a non-monotonic trend with composition. Thickness is measured by ellipsometry, and error bars represent ±1 standard deviation from the average thickness of replicate samples.

Figure 3a, annealing P(S-*r*-MMA) (27:73) and PMMA at 423 K (the same T_{ann} as the other polymers) still showed an increase in h_p for $x_{MMA} > 0.5$, confirming that the non-monotonic trend was not simply due to different T_{ann}.

To better evaluate and understand the composition-dependent adsorption behaviour indicated by h_p, we first compare the homopolymer extremes. Despite different interaction strengths with the substrate resulting from their mechanisms of interaction, PS and PMMA adsorbed layers have h_p values within error of each other (listed in Table 2). We calculated h_p as the average thickness after 15 h annealing time, and it was consistent with h_p estimated from saturated exponential fits to the data[54] (see SI for details and comparison). While adsorption from the melt has been studied for both PS and PMMA, simultaneous study for a direct comparison of their growth has been limited to their flattened sublayers.[39] Experimentally, plateau thickness has been related to radius of gyration (R_g) of PS and degree of polymerization (N) of PMMA by the following scaling relationships:[51,52]

$$h_p(PS) = \alpha R_g \quad (1)$$

$$h_p(PMMA) = \beta N^{1/2} \quad (2)$$

where α and β are scaling constants. We calculated values of α and β for PS and PMMA based on our experimental h_p values and R_g and N derived from measured M_W and M_N, respectively. α_{PS} was within error of that previously calculated for identically-synthesized PS,[§,48] and β_{PMMA} was within range of the β = 0.21 ± 0.05 nm^{-1} scaling reported by Durning et al. for PMMA adsorbed layers.[52] Not only were α_{PS} and β_{PMMA}, listed in Table 2, in line with those reported previously, but they were within error of calculated values of α_{PMMA} and β_{PS}, respectively. The similarities in h_p and its scaling with R_g and N for PS and PMMA confirmed that chain length plays a larger role than polymer-substrate interactions in determining h_p for homopolymers, consistent with theoretical arguments.[52] P(S-*r*-MMA) adsorbed layers did not follow this chain-length controlled behaviour. As shown in Table 2, their β values were almost 50% lower than those of PS and PMMA, indicating that the largely chemistry-independent scaling does not extend to copolymers. This discrepancy merited an examination of the homopolymers in search of behaviour that was not captured by the comparison of their h_p values.

Adsorbed layer architecture and chain conformation studies provided further insight into differences in PS and PMMA adsorbed layers, which were used to better understand copolymer behaviour. Superimposing the structure of the tightly-bound flattened components reported by Jiang *et al.*[39] onto our adsorbed layers, we inferred that the PMMA layer was likely comprised of a larger fraction of tightly adsorbed chains (i.e., a thicker flattened layer). Following this logic, PS and PMMA adsorbed layers reached similar h_p but for different reasons: PMMA formed a denser adsorbed layer (due to its thicker flattened layer) with more chains adsorbed, while PS formed an adsorbed layer with more loosely adsorbed chains and an increased formation of loop and tail structures. This is consistent with the different scaling relationship between h_{ads} and adsorbed amount in different polymers.[69] Simulations reported by Linse and Kallrot further supported this picture, with increasing polymer-substrate interaction strength yielding higher amounts of adsorbed chains and contact points per chain.[70] Their bead-spring model and Monte Carlo simulations also predicted a higher concentration of trains and a lower concentration of tails in polymer chains with higher interaction strength.

Effects of Composition on Growth Kinetics

Adsorption kinetics proved another useful metric by which to compare the impact of polymer-substrate interaction strength on irreversible adsorption of PS and PMMA. While the secondary, slower adsorbed layer growth is generally accepted to proceed logarithmically,[39,50] the initial, fast growth regime has been described to follow either a linear[50,53,54] or power law[39,40] function. Our data showed better agreement with linear growth at short times, following the model proposed by Housmans *et al.*:[50,53]

$$h_{ads}(t) = \begin{cases} h_{t=0} + vt & t < t_{cross} \\ h_{cross} + \Pi \log {}^{t}/_{t_{cross}} & t > t_{cross} \end{cases} \quad (3)$$

where h_{ads} is the adsorbed layer thickness at annealing time t, v and Π are the linear and logarithmic growth rates, and t_{cross} is a crossover time. These kinetic parameters, determined by fitting Equation 3 to the data in Figure 2, are reported in Table 2 with details of the fitting procedure given in the SI. The linear growth rate (v = 0.7 nm/h) that we measured for PS was 2-3 times higher than that reported by Housmans *et al.* for monodisperse PS with the same M_W.[50] We attribute this difference to dispersity effects, with longer chains in the distribution leading to faster adsorption. Although lower molecular weight chains are expected to preferentially adsorb in melt systems due to smaller entropic penalties,[71,72] they would not exclude all high molecular weight chains. Regardless, the similar M_W and $Đ$ of our polymers insured that the derived growth rates were sufficient to compare polymer growth kinetics as a function of composition, without molecular weight effects.

Although the kinetics of PMMA adsorption from the melt has been studied less extensively, it follows a bimodal adsorption pattern from solution[55] that is consistent with the two-stage mechanism proposed for melt adsorption of PS, and Equation 3 has been used to determine its linear growth rate.[53] Adsorption rates, v and Π, are plotted against composition as the open symbols in Figure 3b and c. The slower adsorption of PMMA relative to PS is consistent with both simulation and experimental results. Both Linse and Kallrot's bead-spring model[70] and the study of flattened layers by Jiang *et al.*[39] argued that chains with stronger substrate-interaction strength adsorb more tightly to the substrate, serving as a kinetic barrier to additional adsorption and thereby slowing growth.

As with plateau thickness, the kinetic trends observed for homopolymers could not be directly applied to copolymers,

Table 2 Quantification of adsorbed layer growth.

T_g + 45 K								
Polymer	h_p (nm)	α	β (nm^{-1})	v (nm/h)	h_0 (fit) (nm) §§	t_{cross} (nm)	Π	h_{cross} (nm)
PS	6.0 ± 0.6	0.65 ± 0.07	0.25 ± 0.03	0.8 ± 0.23	1.0 ± 0.5	5	2.4 ± 0.4	4.2 ± 0.1
P(S-*r*-MMA) (75:25)	3.4 ± 0.5	-	0.14 ± 0.02	0.30 ± 0.04	1.2 ± 0.2	6	2.9 ± 0.3	1.8 ± 0.1
P(S-*r*-MMA) (48:52)	2.9 ± 0.5	-	0.13 ± 0.02	0.11 ± 0.01	1.09 ± 0.05	10	1.5 ± 0.3	2.15±0.05
P(S-*r*-MMA) (27:73)	4.1 ± 0.4	-	0.18 ± 0.02	0.2 ± 0.1	1.8 ± 0.4	6	1.1 ± 0.8	3.2 ± 0.5
PMMA	5.9 ± 0.2	0.62 ± 0.02	0.25 ± 0.01	0.34 ± 0.06	1.7 ± 0.2	7	1.6 ± 0.4	5.0 ± 0.2

443 K								
Polymer	h_p (nm)	α	β (nm^{-1})	v (nm/h)	h_0 (fit) (nm)	t_{cross} (nm)	Π	h_{cross} (nm)
PS	7.0 ± 0.5	0.76 ± 0.05	0.29 ± 0.02	3.1 ± 0.3	0 ± 0.1	2	2.8 ± 0.5	4.2 ± 0.4
P(S-*r*-MMA) (75:25)	5.9 ± 0.6	-	0.25 ± 0.03	0.5 ± 0.2	1.8 ± 0.4	6	3 ± 1	4.2 ± 0.6
P(S-*r*-MMA) (48:52)	5.56 ± 0.07	-	0.24 ± 0.01	0.66 ± 0.08	1.3 ± 0.2	5	2.1 ± 0.2	4.15±0.09
P(S-*r*-MMA) (27:73)	5.8 ± 0.6	-	0.25 ± 0.03	1.2 ± 0.2	1.4 ± 0.1	2	0.7 ± 0.6	5.0 ± 0.5
PMMA	6.3 ± 0.5	0.68 ± 0.05	0.27 ± 0.02	2.6± 0.7	1.4 ± 0.4	2	0 ± 0.7	7.1 ± 0.4

Several methods for quantifying the growth patterns for PS and PMMA adsorbed layers exist in the literature and have been applied here to homopolymer and copolymer data sets where possible. Plateau thickness, h_p, was determined from averaging adsorbed layer thickness after 15 h annealing. The values for α and β are scaling factors for R_g and $N^{1/2}$, respectively with respect to h_p. v and Π are the linear and logarithmic growth rates determined by fitting data to the model predicted by Housmans *et al.*[50] h_0 and h_{cross} are the corresponding fitted thicknesses at t_{ads} = 0 and t_{cross}.

and adsorption rate did not slow with increased MMA content. However, while h_p increased symmetrically with increasing compositional homogeneity, kinetics indicated a more biased trend. Apart from (48:52), the other copolymers were both within error of PMMA's linear growth rate, and polymers with x_{MMA} > 0.5 displayed logarithmic growth rates within error of PMMA. These kinetic commonalities between P(S-*r*-MMA) and PMMA suggest a similar growth mechanism and a shared kinetic barrier.

Sensitivity to Annealing Temperature

Comparison of adsorbed layer growth at multiple annealing temperatures provided a means to elucidate the relative temperature-sensitivity of h_p and kinetics, which enabled the isolation of different contributions to adsorption: relative polymer-substrate interaction strength and activation energy of segmental motion.[53] Films were all annealed at 443 K (well above T_g of all polymers) prior to adsorbed layer isolation. Figure 4 illustrates the changes in the resulting adsorbed layer growth patterns, with corresponding h_p and kinetic parameters represented by the solid symbols in Figure 3. The change in annealing temperature (ΔT_{ann}) varied for each polymer, depending on its T_g, and is indicated in Figure 4 caption. It is clear that an increase in T_{ann} led to an overall increase in adsorption kinetics, consistent with previous studies on PS.[50] Interestingly, copolymer adsorbed layers also exhibited an increase in h_p, which is contrary to the results of Simavilla *et al.* for homopolymers.[53]

As indicated in Figure 3a, plateau thicknesses of PS and PMMA did not show large changes with T_{ann}, reflecting the expected behaviour for weakly-temperature dependent polymer-substrate interaction strength (~ k_BT).[50,53] By contrast, P(S-*r*-MMA) showed significant increases in h_p, reaching scaling values within error of β_{PS} and β_{PMMA}. This change in copolymer h_p with T_{ann} indicates a different governing mechanism for copolymer growth where small increases in segmental interaction strength with the substrate can impact h_p.

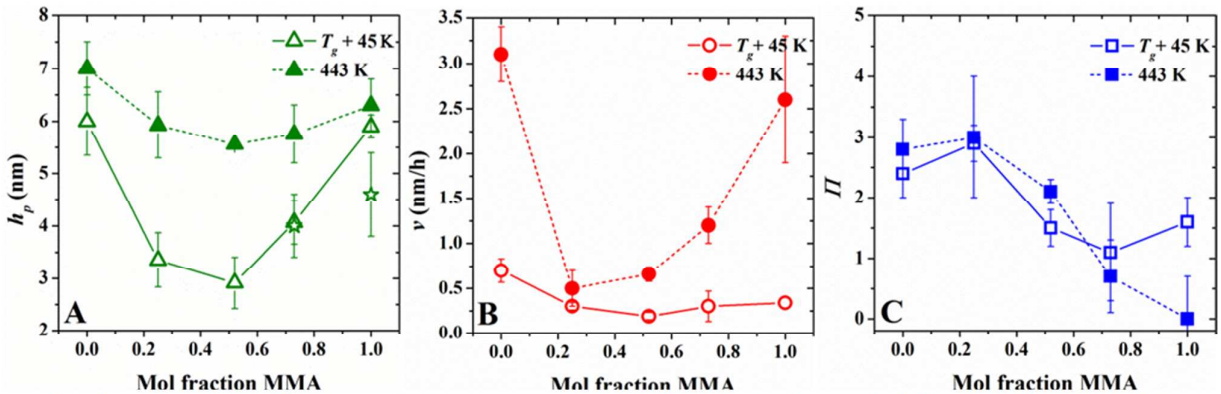

Figure 3. (a) Plateau thickness, h_p, and (b) linear, v, and (c) logarithmic, Π, growth rates of PS, P(S-*r*-MMA), and PMMA adsorbed layers created at T_{ann} = T_g + 45 K (open symbols) and T_{ann} = 443 K (closed symbols). Stars in Figure 3a represent h_p for P(S-*r*-MMA) (73:27) and PMMA created at T_{ann} = 423 K. h_p was calculated by averaging h_{ads} (t_{ads} > 15 h).

Annealing copolymers up to 60 h at T_g + 45 K did not show an increase in adsorbed layer thickness to within range of their h_p at 443 K (see SI), confirming that the low h_p observed at 423 K was not due to slow kinetics masking a later plateau.

Increasing T_{ann} resulted in an overall increase in linear growth rate, with homopolymers exhibiting the largest degree of change. While the increases in v were approximately equal for PS and PMMA, ΔT_{ann} was 20 K for PS and only 5 K for PMMA. The increased temperature sensitivity of v in PMMA was consistent with its higher activation energy of segmental motion (E_a) relative to PS[53,73] and corresponds to a larger increase in molecular motion with temperature, following Arrhenius kinetics.[50,53] The linear growth rate of P(S-*r*-MMA) adsorbed layers increased with MMA content, despite a decreasing ΔT_{ann}, indicating an increase in E_a and temperature-sensitivity with MMA content. Logarithmic growth rates stayed approximately constant with ΔT_{ann} in PS and S-rich copolymers, and they decreased in PMMA and MMA-rich copolymers. We attribute this to the accelerated linear growth of MMA-rich polymers quickly filling surface sites and reducing opportunities for chain diffusion and/or rearrangement, thereby slowing Π.

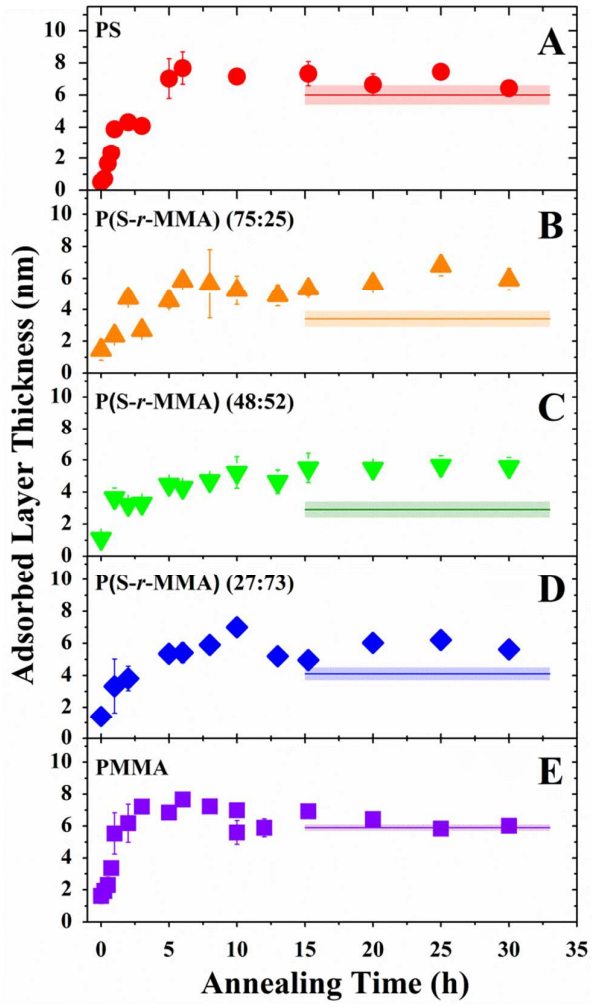

Figure 4. Adsorbed layer growth after annealing films at 443 K reveals composition-dependent changes from those annealed at T_g + 45 K. Thickness plateaus for T_g + 45 K adsorbed layers are shown by the lines for comparison. (A) PS, ΔT_{ann} = 20 K; (B) P(S-*r*-MMA) (75:25), ΔT_{ann} = 20 K; (C) P(S-*r*-MMA) (48:52), ΔT_{ann} = 20 K; (D) P(S-*r*-MMA) (27:73), ΔT_{ann} = 13 K; (E) PMMA, ΔT_{ann} = 5 K.

Proposed P(S-*r*-MMA) Adsorption Mechanism

P(S-r-MMA) possesses characteristics of both PS and PMMA, which manifest as intermediate T_g in bulk systems as well as confined T_g in thin films. However, as shown above, these shared characteristics do not translate directly to adsorbed layer thickness. The illustrations in Figure 5 depict proposed differences in PS and PMMA adsorbed layer chain configuration that combine in their random copolymers. Consistent with experimental observations and simulation results,[39,70] PS (left) adsorbs more loosely due to its relatively weak interaction with the substrate. While still forming a tightly-bound flattened layer,[74,75] it has been previously shown to be thinner,[39] thus allowing more chains to loosely adsorb. These PS chains would also be more able to rearrange at later stages of adsorption, which is reflected in their higher Π. The overall PS adsorbed layer would therefore have a higher concentration of loops and tails compared to that of PMMA (right), which has more tightly adsorbed chains in the form of trains due to stronger polymer-substrate interactions.

In a P(S-*r*-MMA) adsorbed layer (centre), these tendencies for strong and weak chain adsorption from MMA and S contributions combine to increase packing frustration and prevent additional chain adsorption. The stronger MMA interactions dictate chain conformations close to the substrate, leading to tighter adsorption and a thicker flattened layer that increases the barrier for additional adsorption, slowing kinetics consistent with the similarities in kinetics with PMMA. Chain packing frustration from different interaction strengths at the substrate could also contribute to kinetic barriers. Simultaneously, the S fraction contributes toward weaker average segmental attraction to the substrate, which, combined with a thicker flattened layer, does not allow many chains to penetrate to the surface and loosely adsorb. With limited adsorption of loosely-bound chains, P(S-*r*-MMA) adsorbed layers would not greatly exceed the thickness of their flattened layer and form thinner adsorbed layers than their homopolymer components. In PMMA, individual segments have interactions strong enough to diffuse through denser, tightly-bound chains to adsorb. In PS, weaker-adsorbing chains are less encumbered by the flattened layer, and chains form more loops and tail configurations. This competition between tight and loose chain adsorption increases with increasing compositional heterogeneity. Unbalanced compositions in P(S-*r*-MMA) (27:73) and (75:25) allowed MMA and S units to dominate the adsorption mechanism, respectively, resulting in larger h_p. However, the nearly symmetric composition of P(S-*r*-MMA) (48:52) led to the most dramatic competition of influences and was thinner accordingly. The different structures of copolymer adsorbed layers explain proportionality differences between h_{ads} and

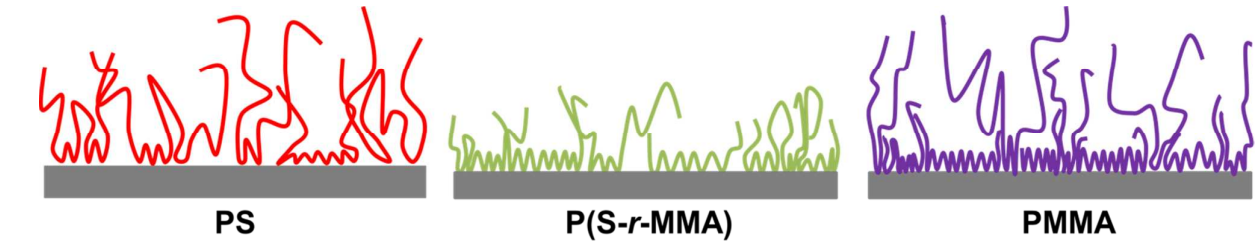

Figure 5. Diagram of proposed differences between PS, PMMA, and P(S-*r*-MMA) adsorbed layers. PS exhibits loser adsorption, with more loops and tails. PMMA has tighter chain adsorption, but also many loosely-adsorbed chains with only a few contact points. P(S-*r*-MMA) has tighter bound chains than PS, giving it less large loops and tails, but it also does not have the loosely-bound chains in gaps in the tightly bound layer that PMMA does.

adsorbed amount. This likely accounts for the different trends between deviations from bulk T_g under confinement[9,32] and h_p with composition.

Finally, the temperature-sensitivity of copolymer adsorption is consistent with this proposed mechanism. The large change in copolymer h_p at elevated T_{ann} indicated a change in polymer-substrate interaction strength and supports the idea of limited loosely bound chain adsorption. In copolymers, this small increase in ~k_BT interactions allows for the penetration of additional chains through the tightly-bound layer to bind with the substrate. However, the fact that P(S-*r*-MMA) (27:73) did not show a change in h_p when created at T_{ann} = 423 K implies that a sufficiently high T_{ann} is needed to overcome the barrier to adsorption imposed by tightly bound chains. The relatively small change in copolymer *v* demonstrated that the thermal fluctuation of chains played a less important role in limiting adsorption than interaction energy with the substrate.

Conclusions

Through the examination of adsorbed layer growth in PS, PMMA, and a series of their random copolymers, we gained a clearer picture of how different polymer-substrate interactions combine to influence irreversible adsorption in systems with compositional heterogeneity. Our results revealed that the irreversible adsorption of P(S-*r*-MMA) faces additional barriers to growth than either of its component homopolymers and is not intermediate to their two behaviours. This differed substantially from the blended properties usually displayed by random copolymers, which extend to their confined T_g behavior.[9,32] Kinetic analysis confirmed that tightly binding chains dictate copolymer adsorption rates, as in PMMA. Annealing at a higher temperature increased kinetics and enabled the recovery of copolymer h_p scaling consistent with homopolymers.

These insights provided a picture of P(S-*r*-MMA) adsorption where tighter adsorption and weaker average individual interaction strengths resulting from compositional heterogeneity combine to limit the adsorption of loosely-bound chains and give thinner adsorbed layers. P(S-r-MMA) formed thicker tightly-bound layers at the substrate than PS, which served as a barrier to additional adsorption of chains with weaker average segment-substrate interactions than PMMA. Raising T_{ann} increased the segmental attraction to the substrate sufficiently to overcome the growth barrier imposed by the tightly-bound layer and allowed for additional chains to be adsorbed.

Differences between confined T_g and adsorption trends suggest that polymer-substrate interactions are not sufficient to predict adsorption of compositionally-complex systems. Their reduced adsorbed layer thickness implies that P(S-*r*-MMA) films are less susceptible to annealing-induced property changes, providing copolymerization as a route to reducing processing effects on thin film behaviour. However, in order to directly connect our results to changes in film properties, additional information is needed to determine precisely how h_{ads} translates to adsorbed amount in copolymers. Work should also be undertaken to determine if copolymers with similar polymer-substrate interactions show inhibited adsorption.

Conflicts of interest

There are no conflicts to declare

Acknowledgements

R.D.P. acknowledges the support of the National Science Foundation (NSF) Materials Research Science and Engineering Center Program through the Princeton Center for Complex Materials (DMR-1420541) and the AFOSR through a PECASE Award (FA9550-15-1-0017).

Notes and references

‡ Tacticity-dependent confinement behavior has been attributed to the degree of hydrogen bonding with the substrate allowed by the relative proximity of carbonyl groups to the native oxide layer.[68] From preliminary experiments and studies of spin-coated PMMA on Al,[76] we expect tacticity also influences PMMA's affinity for irreversible adsorption. The PMMA used here has a 4:37:59 isotactic:atactic:syndiotactic triad ratio, as determined by ^{1}H-NMR (see SI), which is consistent with what is expected for PMMA synthesized via free radical polymerization in bulk.[77,78]

§ α_{PS} calculated is higher than the α = 0.47 reported by Fujii *et al.* for monodisperse PS.[51] This difference is likely due to the broader distribution of chain lengths in our polymer not being fully captured

by average R_g and disproportionally contributing to h_p. Since h_p increases with molecular weight,[51] it follows that longer chains likely increase h_p, resulting in a larger α.

§§ The initial thickness at $t_{ads} = 0$ (h_o) was fitted to the data and fell within error of experimentally-measured thicknesses without annealing.

1 J. Pye, K. Rohald, E. Baker, and C. Roth, *Macromolecules*, 2010, **43,** 8296.
2 R. Priestley, C. Ellison, L. Broadbelt, and J. Torkelson, *Science*, 2005, **309,** 456.
3 C. Zhang, V. Boucher, D. Cangialosi, and R. Priestley, *Polymer*, 2013, **54,** 230.
4 C. Stafford, C. Harrison, K. Beers, A. Karim, E. Amis, M. VanLandingham, H. Kim, W. Volksen, R. Miller, and E. Simonyi, *Nat. Mater.*, 2004, **3,** 545.
5 J. Torres, C. Wang, B. Coughlin, J. Bishop, R. Register, R. Riggleman, C. Stafford, and B. Vogt, *Macromolecules*, 2011, **44,** 9040.
6 C. Stafford, B. Vogt, C. Harrison, D. Julthongpiput, and R. Huang, *Macromolecules,* 2016, **39,** 5095.
7 M. Zhang, S. Askar, J. Torkelson, and L. Brinson, *Macromolecules*, 2017, **50**, 5447.
8 B. Vogt, *J. Polym. Sci. Part B: Polym. Phys.*, 2018, **56,** 9.
9 M. Mundra, C. Ellison, R. Behling, and J. Torkelson, *Polymer*, 2006, **47,** 7747.
10 S. Kim, S. Hewlett, C. Roth, and J. Torkelson, *Eur. Phys. J. E: Soft Matter Biol. Phys.*, 2009, **30,** 83.
11 C. Ellison, J. Torkelson, *Nat. Mater.,* 2003, **2,** 695.
12 J. Keddie, R. Jones, and R. Cory, *Europhys. Lett.*, 1994, **27,** 59.
13 J. Forrest, K. Dalnoki-Veress, J. Stevens, and J. Dutcher, *Phys. Rev. Lett.*, 1996, **77,** 2002.
14 H. Park, J. Kamcev, L. Robeson, M. Elimelech, and B. Freeman, *Science*, 2017, **356,** 1137.
15 E. Jackson, and M. Hillmyer, *ACS Nano*, 2010, **4,** 3548.
16 C. Bates, M. Maher, D. Janes, C. Ellison, and C. Willson, *Macromolecules*, 2014, **47,** 2.
17 C. Hardy and C. Tang, *J. Polym. Sci. Part B: Polym. Phys.*, 2013, **51,** 2.
18 S. Yang, J, Yang, E. Kim, G. Jeon, E. Oh, K. Choi, S. Hahn, and J. Kim, *ACS Nano*, 2010, **4,** 3817.
19 O. Bäumchen, J. McGraw, J. Forrest, and K. Dalnoki-Veress, *Phys. Rev. Lett.*, 2012, **109,** 55701.
20 S. Kim, and J. Torkelson, *Macromolecules*, 2011, **44,** 4546.
21 R. Baglay, and C. Roth, *J. Chem. Phys.*, 2015, **143,** 111101.
22 R. Baglay, and C. Roth, *J. Chem. Phys.*, 2017, **146,** 203307.
23 J. Keddie, R. Jones, and R. Cory, *Faraday Discuss.*, 1994, **98,** 219.
24 J. Sharp, and J. Forrest, *Phys. Rev. Lett.*, 2003, **91,** 235701.
25 M. Ediger, and J. Forrest, *Macromolecules,* 2014, **47,** 471.
26 R. Priestley, M. Mundra, N. Barnett, L. Broadbelt, and J. Torkelson, *Aust. J. Chem.,* 2007, **60,** 765.
27 C. Ellison, M. Mundra, and J. Torkelson, *Macromolecules*, 2005, **38,** 1767.
28 C. Roth, K. McNerny, W. Jager, and J. Torkelson, *Macromolecules*, 2007, **40,** 2568.
29 K. Paeng, R. Richert, and M. Ediger, *Soft Matter*, 2011, **8,** 819.
30 Z. Fakhraai, and J. Forrest, *Science,* 2008, **319,** 600.
31 C. Roth, A. Pound, S. Kamp, C. Murray, and J. Dutcher, *Eur. Phys. J. E: Soft Matter Biol. Phys.*, 2006, **20,** 441.
32 C. Park, J. Kim, M. Ree, B. Sohn, J. Jung, and W. Zin, *Polymer,* 2004, **45,** 4507.
33 J. Chung, T. Chastek, M. Fasolka, H. Ro, and C. Stafford, *ACS Nano*, 2009, **3,** 844.
34 A. Panagopoulou and S. Napolitano, *Phys. Rev. Lett.*, 2017, **119,** 097801.
35 C. Rotella, S. Napolitano, and M. Wübbenhorst, *Macromolecules*, 2009, **42,** 1415.
36 S. Napolitano, *Non-equilibrium Phenomena in Confined Soft Matter: Irreversible Adsorption, Physical Aging, and Glass Transition at the Nanoscale*, Springer, Cham, 2015.
37 S. Napolitano, S. Capponi, and B. Vanroy, *Eur. Phys. J. E: Soft Matter Biol. Phys.*, 2013, **36,** 1.
38 S. Napolitano and M. Wübbenhorst, *Nat. Commun.*, 2011, **2,** 260.
39 N. Jiang, J. Shang, X. Di, M. Endoh, and T. Koga, *Macromolecules*, 2014, **47,** 2682.
40 P. Gin, N. Jiang, C. Liang, T. Taniguchi, B. Akgun, S. Satija, M. Endoh, and T. Koga, *Phys. Rev. Lett.*, 2012, **109,** 265501.
41 N. Jiang, L. Sendogdular, X. Di, M. Sen, P. Gin, M. Endoh, T. Koga, B. Akgun, M. Dimitriou, and S. Satija, *Macromolecules*, 2015, **48,** 1795.
42 C. Rotella, S. Napolitano, L. De Cremer, G. Koeckelberghs, and M. Wübbenhorst, *Macromolecules*, 2010, **43,** 8686.
43 J. Xu, Z. Liu, Y. Lan, B. Zuo, X. Wang, J. Yang, W. Zhang, and W. Hu, *Macromolecules,* 2017, **50,** 6804.
44 T. Koga, N. Jiang, P. Gin, M. Endoh, S. Narayanan, L. Lurio, and S. Sinha, *Phys. Rev. Lett.*, 2011, **107,** 225901.
45 S. Napolitano, C. Rotella, and M. Wübbenhorst, *ACS Macro Lett.*, 2012, **1,** 1189.
46 N. Jiang, M. Sen, M. Endoh, T. Koga, E. Langhammer, P. Bjöörn, and M. Tsige, *Langmuir*, 2018, **34,** 4199.
47 S. Sun, H. Xu, J. Han, Y. Zhu, B. Zuo, X. Wang, and W. Zhang, *Soft Matter,* 2016, **12,** 8348.
48 M. Burroughs, S. Napolitano, D. Cangialosi, D. and R. Priestley, *Macromolecules*, 2016, **49,** 4647.
49 N. Perez-de-Eulate, M. Sferrazza, D. Cangialosi, and S. Napolitano, *ACS Macro Lett.*, 2017, **6,** 354.
50 C. Housmans, M. Sferrazza, and S. Napolitano, *Macromolecules*, 2014, **47,** 3390.
51 Y. Fujii, Z. Yang, J. Leach, H. Atarashi, K. Tanaka, and O. Tsui, *Macromolecules*, 2009, **42,** 7418.
52 C. Durning, B. O'Shaughnessey, U. Sawhney, D. Nguyen, J. Majewski, and G. Smith, *Macromolecules*, 1999, **32,** 6772.
53 D. Simavilla, W. Huang, P. Vandestrick, J. Ryckaert, M. Sferrazza, and S. Napolitano, *ACS Macro Lett.*, 2017, **6,** 975.
54 D. Simavilla, A. Panagopoulou, and S. Napolitano, *Macromol. Chem. Phys.*, 2017, **219,** 1700303.
55 H. Schneider, P. Frantz, and S. Granick, *Langmuir*, 1996, **12,** 994.
56 H. Johnson, J. Douglas, and S. Granick, *Phys. Rev.*, 1993, **70,** 3291.
57 H. Johnson, and S. Granick, *Macromolecules*, 1990, **23,** 3367.
58 P. Mansky, Y. Liu, E. Huang, T. Russell, and C. Hawker, *Science*, 1997, **275,** 1458.
59 S. Pujari, M. Keaton, P. Chaikin, and R. Register, *Soft Matter*, 2012, **8,** 5358.
60 M. Coote, L. Johnston, and T. Davis, *Macromolecules*, 1997, **30,** 8191.
61 W. Bushuk, and H. Benoit, *Can. J. Chem.*, 1958, **36,** 1616.
62 D. Christie, R. Register, and R. Priestley, *ACS Cent. Sci.*, 2018, **4**, 504.
63 A. Burns, and R. Register, *Macromolecules*, 2016, **49,** 269.
64 C. Brazel, and S. Rosen, *Fundamental Principles of Polymeric Materials*, Wiley, Hoboken, NJ, Third Ed., 2012.
65 B. Zhang, and F. Blum, *Macromolecules*, 2003, **36,** 8522.
66 G. Liu, Z. Meng, W. Wang, Y. Zhou, and L. Zhang, *J. Phys. Chem. B*, 2008, **112,** 93.
67 G. Liu, L. Zhang, Y. Yao, L. Yang, and J. Gao, *J. Appl. Polym. Sci.*, 2003, **88,** 2891.
68 Y. Grohens, L. Hamon, G. Reiter, and A. Soldera, and Y. Holl, *Eur. Phys. J. E: Soft Matter Biol. Phys.*, 2002, **8,** 217.
69 D. Simavilla, W. Huang, C. Housmans, M. Sferrazza, and S. Napolitano, *ACS Cent. Sci.,* 2018, **4,** 755.

70 P. Linse, and N. Kallrot, *Macromolecules*, 2010, **43,** 2054.
71 J. Van der Gucht, N. Besseling, and G. Fleer, *Macromolecules*, 2002, **35,** 6732.
72 J. Van Der Gucht, N. Besseling, and G. Fleer, *Macromolecules,* 2004, **37,** 3026.
73 L. Manring, *Macromolecules,* 1988, **21,** 528.
74 M. Sen, N. Jiang, J. Cheung, M. Endoh, T. Koga, D. Kawaguchi, and K. Tanaka, *ACS Macro Lett.*, 2016, **5,** 504.
75 M. Sen, N. Jiang, M. Endoh, T. Koga, A. Ribbe, A. Rahman, D. Kawaguchi, K. Tanaka, and D. Smilgies, *Macromolecules*, 2018, **51,** 520.
76 Y. Grohens, M. Brogly, C. Labbe, and J. Schultz, *Polymer*, 1997, **38,** 5913.
77 Y. Isobe, K. Yamada, T. Nakano, and Y. Okamoto, *J. Polym. Sci. Part A: Polym. Chem.*, 2000, **38,** 4693.
78 R. Kirste, W. Kruse, and K. Ibel, *Polymer,* 1975, **16,** 120.

Table of Contents Entry

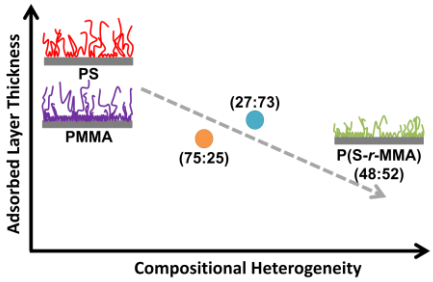

Compositional heterogeneity introduces a competition between individual polymer-substrate interactions that limits the growth of irreversibly adsorbed layers.